

## Observation of a Nonlocal Conductivity in the Mixed State of $\text{YBa}_2\text{Cu}_3\text{O}_{7-\delta}$ : Experimental Evidence for a Vortex Line Liquid

H. Safar, P. L. Gammel, D. A. Huse, S. N. Majumdar, L. F. Schneemeyer, and D. J. Bishop  
*AT&T Bell Laboratories, Murray Hill, New Jersey 07974*

D. López, G. Nieva, and F. de la Cruz  
*Centro Atómico Bariloche, 8400 San Carlos de Bariloche, Argentina*  
(Received 10 September 1993)

We report on transport measurements in the mixed state of  $\text{YBa}_2\text{Cu}_3\text{O}_7$  single crystals using the dc flux transformer geometry. In the vortex fluid regime we have observed the onset of a nonlocal conductivity. At lower temperatures, close to but above the phase transition temperature the vortices become effectively three dimensional in character. This is in sharp contrast to recent flux transformer experiments on  $\text{Bi}_2\text{Sr}_2\text{CaCu}_2\text{O}$  which have failed to see a nonlocal conductivity, confirming the two-dimensional character at high temperatures of the vortices in that system. These observations suggest that in a finite temperature interval, the vortex state in  $\text{YBa}_2\text{Cu}_3\text{O}_7$  is a line liquid.

PACS numbers: 74.60.Ge, 74.72.Bk

The magnetic phase diagram of the oxide superconductors is a rich system with many novel physical phenomena playing a significant role. Effects such as thermal fluctuations, disorder, anisotropy, and dimensionality are all important in explaining the experimentally observed behavior [1]. It is now clear from experiments that there is a phase transition in the mixed state which separates a low temperature ordered phase from a high temperature vortex fluid. In the limit of strong pinning disorder, this low temperature phase appears to be a vortex glass [2] and the phase transition is known to be second order [3]. In the weak pinning limit, the low temperature phase is a vortex lattice with long-ranged positional order and the transition is theoretically [4] and experimentally [5] found to be first order. However, there remain many open and important questions regarding the role of the dimensionality of the vortices.

In a layered superconductor with the magnetic field perpendicular to the layers, one may ask whether the vortices in the different layers will tend to align forming vortex lines. This should occur when the interactions between vortices in adjacent layers are not overwhelmed by either thermal fluctuations or random pinning in the layers [2,6]. When the vortices do form lines this reflects strong correlations between layers and so the material is behaving three dimensionally. However, as the temperature is increased, the thermal fluctuations may destroy the correlations between layers [7], breaking the vortex lines up into point or "pancake" vortices in each layer [8] and causing a crossover to two-dimensional behavior. In  $\text{YBa}_2\text{Cu}_3\text{O}_7$  (YBCO) this crossover occurs in the vortex liquid regime and can be studied in a new way using multiterminal transport measurements as reported and analyzed in this Letter.

In this paper, we present transport measurements on YBCO in the vortex liquid regime using the modified dc flux transformer geometry [9]. We show that the data are highly inconsistent with the material being simply an anisotropic, local conductor. Thus we report the first observation of nonlocal conductivity in the mixed state of an

oxide superconductor. This observation allows us to "measure" the vortex dimensionality as a function of temperature and directly show that at a temperature close to but above the vortex phase transition temperature, the vortices become lines that maintain their integrity across samples of thicknesses of 30  $\mu\text{m}$  or more. As suggested by Nelson and co-workers [10], the vortex state in this temperature interval can then be best described as that of a line liquid as opposed to a liquid of pancake vortices which is the appropriate description of the system at higher temperatures. It will presumably be in this line liquid regime that entanglement effects could become important.

The geometry used in this experiment is similar to that previously used both by us [9] and independently by Busch *et al.* [11] in showing that the vortices in  $\text{Bi}_2\text{Sr}_2\text{CaCu}_2\text{O}$  (BSCCO) are two dimensional at high temperatures. It is a modification of the geometry of the flux transformer of Giaever [12] in which the strong anisotropy in the conductivity in the oxide superconductors produces a very nonuniform current distribution in the sample which is the key to seeing the nonlocal effects. In particular, the small  $c$  axis conductivity in comparison to the  $a$ - $b$  plane conductivity means that when the current is injected into contacts at the top of the sample, a substantially higher current flows in the top layers than in the bottom ones. When, in spite of this nonuniform current, we observe the same nonzero voltage drop along the top and bottom of the sample, this indicates that the conductivity is nonlocal and that there is a strong correlation between the motion of vortices at the top and bottom of the sample.

Our samples were single crystals of YBCO which were contacted with eight contacts as shown in the inset in Fig. 1. The crystals were grown using a flux growth technique as described previously. Typical sample dimensions were 1 mm  $\times$  0.5 mm  $\times$  0.03 mm with the small dimension along the  $c$  axis. The samples were heavily twinned with the average distance between twin domain boundaries being  $\sim 1000$  Å. Typical distance between contacts is 0.17

mm, and the contact size is 0.3 mm×0.4 mm. The normal state resistivities of our samples (at 100 K) were typically  $\rho_c = 8 \times 10^{-3} \Omega \text{ cm}$  and  $\rho_{ab} = 6 \times 10^{-5} \Omega \text{ cm}$  as extracted from the measured resistances using a modified Montgomery [13] analysis as will be described below. The samples typically had sharp  $T_c$ 's in the range 91–94 K with the 10%–90% width being  $\sim 0.3 \text{ K}$  wide. We report on measurements of a total of six samples. As will be clear below, we need to introduce a special notation for our voltage measurements. We call  $V_{ab}(I_{cd})$  the voltage measured between terminals  $a$  and  $b$  with the current applied between terminals  $c$  and  $d$ .

Shown in Fig. 1 are typical results for our experiment. Shown are the measured values of  $V_{23}(I_{14})$  and  $V_{67}(I_{14})$  in the linear, Ohmic regime for sample 1 with a thickness of 35  $\mu\text{m}$  with fields applied parallel to the  $c$  axis of 0 and 5 T. In the normal state  $V_{23}(I_{14}) \neq V_{67}(I_{14})$  because of the strong anisotropy with  $\rho_c \gg \rho_a \sim \rho_b$ . As we will show, the response in the normal state can be quantitatively fit using a Montgomery type of analysis which assumes a local conductivity (i.e., that the local electric field is determined simply by the local current density). As the temperature is reduced and we go well into the vortex liquid regime,  $V_{23}(I_{14})$  begins to approach  $V_{67}(I_{14})$  and finally at and below a temperature we call  $T_{th}$  we find that  $V_{23}(I_{14}) = V_{67}(I_{14})$ . For larger values of the applied field,  $T_{th}$  occurs at lower temperatures. This behavior is very different from that seen in similar experiments on the much more anisotropic system  $\text{Bi}_2\text{Sr}_2\text{CaCu}_2\text{O}$  (Bi:2212) [9,11], where it was found that the ratio of  $V_{23}(I_{14})/V_{67}(I_{14})$  diverged as the mixed state was entered and continued to diverge as the temperature was lowered. For Bi:2212, throughout the entire temperature-field range studied, the measured values of  $V_{23}(I_{14})/V_{67}(I_{14})$  were far from unity and more importantly could be consistently fit within a Montgomery type

of analysis which assumes local electrostatics. This analysis showed that the vortices were two dimensional in character in that the motion of vortices on the top layer of a macroscopic sample did not induce any measurable evidence of vortex motion on the bottom of the sample. These experiments lent credence to the idea that at high temperatures the vortices in this system are two-dimensional pancake vortices or at least that flux cutting and recombination can happen very easily. In contrast, our measurements in YBCO show that at  $T_{th}$   $V_{23}(I_{14}) = V_{67}(I_{14})$  which suggests that for temperatures below this temperature there is strongly correlated vortex motion across the 35  $\mu\text{m}$  thick sample. As we will show, near and below this temperature the data cannot be consistently fit within the framework of a Montgomery type of analysis which shows that nonlocal effects [14] become important in the measured resistivities.

The identification of  $T_{th}$  as the temperature where thermal fluctuations decorrelate vortex motion across the thickness of the sample suggests that there should be a systematic variation of  $T_{th}$  with sample thickness. Shown in the inset of Fig. 1 are the results of such a study at 1 T. A clear trend of  $T_{th}$  moving to lower temperatures for thicker samples can be seen.

All of the data presented so far have been in the linear response regime. The observation of correlated vortex motion in our samples for temperatures below  $T_{th}$  also raises the possibility of seeing current-induced flux cutting below this temperature as opposed to the thermal fluctuation-induced effects we have already presented. Shown in Fig. 2 are data from a series of experiments studying the nonlinear effects below  $T_{th}$ . Shown are measured values of  $V_{23}(I_{14})$  and  $V_{67}(I_{14})$  for a 32  $\mu\text{m}$  thick

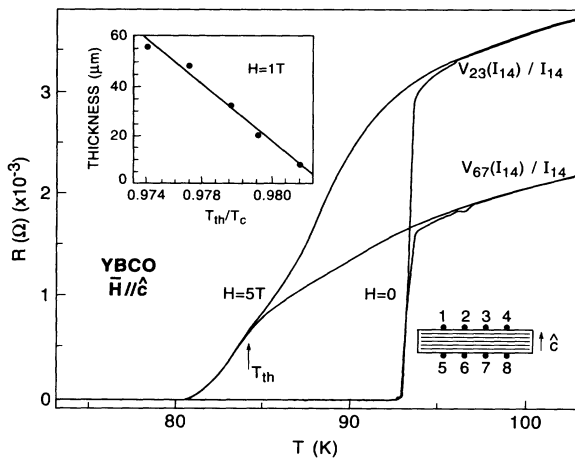


FIG. 1. Shown are the measured temperature dependences of  $V_{23}(I_{14})/I_{14}$  and  $V_{67}(I_{14})/I_{14}$  for applied fields of 0 and 5 T. In the inset is shown the thickness dependence of  $T_{th}$  for an applied field of 1 T. The sample geometry is also shown.

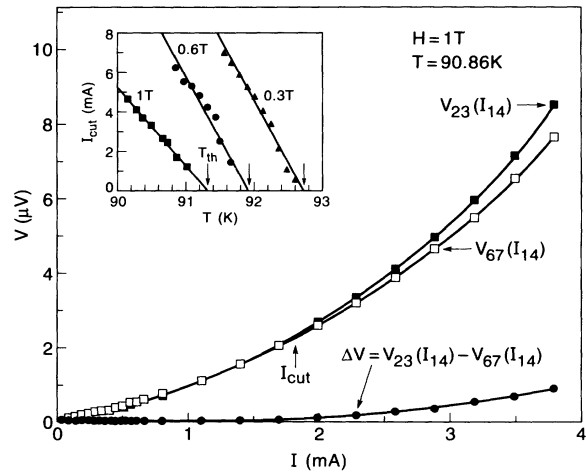


FIG. 2. Shown are  $V_{23}(I_{14})$  and  $V_{67}(I_{14})$  as a function of measuring current  $I_{14}$ . Also shown is  $\Delta V = V_{23}(I_{14}) - V_{67}(I_{14})$ . In the inset is shown the temperature dependence of  $I_{cut}$  which is defined in the figure as the current where  $V_{23}(I_{14}) = V_{67}(I_{14})$ . The arrows show the independently measured values of  $T_{th}$  for the various applied fields.

sample as a function of measuring current  $I_{14}$  at a field of 1 T for a temperature which is below  $T_{th}$  for this sample and field. For low measuring currents  $V_{23}(I_{14}) = V_{67}(I_{14})$  below  $T_{th}$ . However, for measuring currents beyond some value  $I_{cut}$ , we find  $V_{23}(I_{14}) > V_{67}(I_{14})$ . Shown in the inset of Fig. 2 is the temperature dependence of  $I_{cut}$  for three different applied fields. Also shown as the arrows are the independently measured, low current values of  $T_{th}$  which agree well with the extrapolation to zero of the measured values of  $I_{cut}$ . These data suggest that, for large vortex driving forces on the top face of the sample, there is enough vortex tearing or cutting and recombination that there is no correlated motion on the bottom of the sample. However, if the vortices on the top of the sample are pulled sufficiently slowly, then the entire vortex array can be made to move as one with the same speed on the top and bottom of the sample as indicated by  $V_{23}(I_{14}) = V_{67}(I_{14})$ .

The identification of  $T_{th}$  as the temperature where there is significant correlated vortex motion across the thickness of a macroscopic sample also suggests that one should be able to see nonlocal effects in the transport at and above this temperature. In the final section of this paper we will show that even above  $T_{th}$  nonlocal effects can become very important in the measured values of the anisotropic resistivities. We will do this by following the argument of Huse and Majumdar [14] which proceeds as follows: Consider two different types of experiments that one can do to probe the anisotropic resistivities in this system. The first has been shown in Fig. 1. In that experiment, the current is injected primarily parallel to the  $a$ - $b$  planes (into contact 1 and out of contact 4). The second type of experiment is shown in the inset of Fig. 3. There the current is injected primarily parallel to the  $c$  axis (into contact 1 and out of contact 5). In both experiments the field is applied parallel to the  $c$  axis and the

resistances are measured in the linear, Ohmic regime. The proof of nonlocality will proceed as follows. Each of the two experiments can be fit *separately* within a Montgomery type of analysis which assumes only an anisotropic local conductivity and the validity of linear response. However, as we will show, in the mixed state, at and above  $T_{th}$ , the apparent anisotropies resulting from such an analysis are quite different for the two experiments. This is evidence of the breakdown of the assumption of locality for the mixed state.

For example, in Fig. 1, as the temperature is reduced to  $T_{th}$ , the ratio  $V_{23}(I_{14})/V_{67}(I_{14})$  approaches 1. In a local conductor this will only occur if  $\rho_c$  is dropping faster than  $\rho_{ab}$ . The Montgomery analysis of an anisotropic local conductor can be generalized to this geometry [15] and the apparent conductivity ratio ( $\rho_c/\rho_{ab}$ ) extracted from the analysis. Shown in Fig. 4 is the result of that analysis. As expected, the quantitative result shows an apparent ( $\rho_c/\rho_{ab}$ ) essentially constant above  $T_c$  and *dropping rapidly* below  $T_c$ .

In Fig. 3 are the data from the other experiment. Shown are the ratios  $V_{37}(I_{15})/V_{26}(I_{15})$ ,  $V_{48}(I_{15})/V_{37}(I_{15})$ , and  $V_{48}(I_{15})/V_{26}(I_{15})$  measured with the current flowing primarily parallel to the  $c$  axis. The data in Fig. 3 show these ratios also approaching 1 as  $T_{th}$  is approached from above. This will occur in a local conductor only if  $\rho_{ab}$  is dropping faster than  $\rho_c$ , in stark contrast to the previous result. Shown in Fig. 4 are the quantitative results of the closed form analysis of this experiment. As expected the quantitative analysis of this experiment results in an apparent  $\rho_c/\rho_{ab}$  which is nearly independent of temperature above  $T_c$  and which *diverges* near  $T_{th}$ . The quantitative analysis of the two experiments produces values of  $\rho_c/\rho_{ab}$  which agree to within 10% above  $T_c$  but which are different by more than 6 orders of magnitude as one approaches  $T_{th}$ . This huge discrepancy between the results of two experiments whose

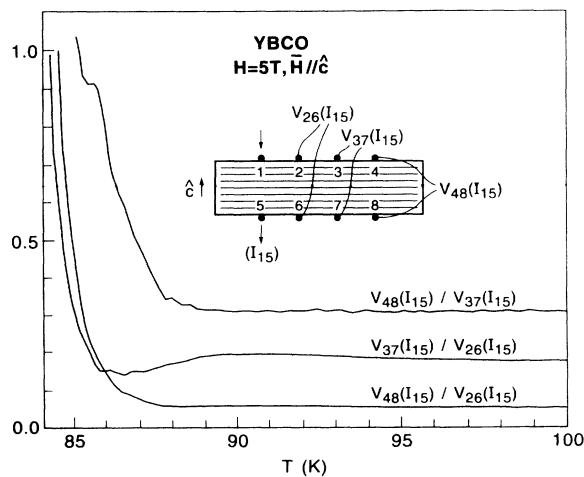


FIG. 3. Shown are the measured temperature dependences of the ratios  $V_{37}(I_{15})/V_{26}(I_{15})$ ,  $V_{48}(I_{15})/V_{37}(I_{15})$ , and  $V_{48}(I_{15})/V_{26}(I_{15})$ . The drawing shows the sample geometry.

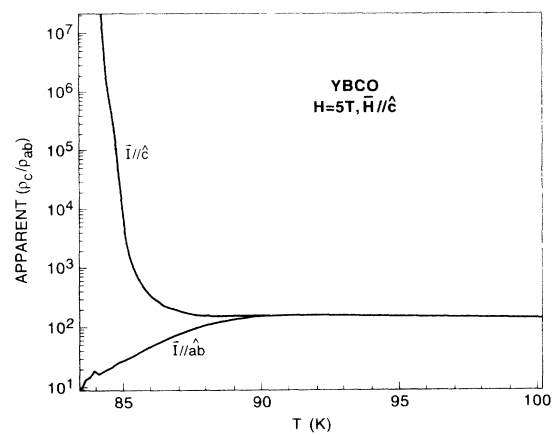


FIG. 4. Shown are the apparent values of the ratio  $\rho_c/\rho_{ab}$  as extracted from the two experiments shown in the insets of Fig. 1 and Fig. 3.

analysis only assumes a local conductivity shows clearly where nonlocal effects come into play in transport in the mixed state in this system. We emphasize that the other major assumption implicit in the Montgomery analysis, the validity of linear response, has been experimentally checked for and all of the data shown in Fig. 4 are well within the linear regime [16].

The data in this paper provide a microscopic explanation of the ubiquitous shoulder always seen in the resistance in the mixed state in YBCO. Our measurements suggest that this shoulder is where there is a two- to three-dimensional crossover in the dimensionality of the vortices in this system. This explanation is qualitatively consistent with measurements made in artificial multilayers [17] where a similar feature is seen in the resistance and for which convincing evidence has been obtained for a two- to three-dimensional crossover at that point for the vortices in that system. Our observations also provide a microscopic explanation for a number of other experimental observations made in YBCO. Experiments by Kwok *et al.* [18] have shown that this shoulder marks the onset of the importance of twin boundary pinning. Experiments by Civale *et al.* [19] have also shown that this feature marks the maximum temperature to which the irreversibility line can be shifted upward in the presence of columnar defects. Both observations can be explained as showing that extended defects much more readily pin three-dimensional vortex lines as opposed to two-dimensional vortex pancakes. Finally, our observations show that the first and second order phase transitions in YBCO, for which there exists so much compelling experimental evidence, only occur for three-dimensional vortices.

In conclusion, we report on multiterminal measurements in the mixed state of YBCO. We have provided evidence for nonlocal transport which indicates that there can be strongly correlated vortex motion over macroscopic distances in this system. We have shown that this correlated vortex motion can be destroyed by either thermal fluctuations or the application of large driving forces. These observations provide a natural microscopic explanation for a number of other experimental results obtained in the YBCO system. Finally, our measurements show how, in the presence of nonlocal effects, the local electric field in a superconductor can be determined not just by the local current, but by currents tens of microns away exerting Lorentz forces on very distant sections of vortex lines. It remains a substantial theoretical and experimental challenge to develop a good quantitative understanding of the transport properties in this highly nonlocal regime.

We acknowledge useful discussions with E. Rodriguez, D. R. Nelson, C. Balseiro, and D. S. Fisher, and support from Fundación Antorchas and CONICET, Argentina.

- [1] For a review see, D. J. Bishop, P. L. Gammel, D.A. Huse, and C. A. Murray, *Science* **255**, 165 (1992).  
 [2] D. S. Fisher, M. P. A. Fisher, and D. A. Huse, *Phys. Rev. B* **43**, 130 (1991).  
 [3] R. H. Koch *et al.*, *Phys. Rev. Lett.* **63**, 1511 (1989); P. L. Gammel, L. F. Schneemeyer, and D. J. Bishop, *Phys. Rev. Lett.* **66**, 953 (1991).  
 [4] R. E. Hetzel, A. Sudbø, and D. A. Huse, *Phys. Rev. Lett.* **69**, 518 (1992).  
 [5] H. Safar *et al.*, *Phys. Rev. Lett.* **69**, 824 (1992); W. K. Kwok *et al.*, *Phys. Rev. Lett.* **69**, 3370 (1992).  
 [6] L. I. Glazman and A. E. Koshelev, *Phys. Rev. B* **43**, 2835 (1991); M. V. Feigelman, V. G. Geshkenbein, and A. I. Larkin, *Physica (Amsterdam)* **167C**, 177 (1990).  
 [7] C. Durán *et al.*, *Phys. Rev. B* **44**, 7737 (1991); J. Yazzi *et al.*, *Physica (Amsterdam)* **184C**, 254 (1991).  
 [8] J. R. Clem, *Phys. Rev. B* **43**, 7837 (1991).  
 [9] H. Safar *et al.*, *Phys. Rev. B* **46**, 14238 (1992).  
 [10] D. R. Nelson and H. S. Seung, *Phys. Rev. B* **39**, 9153 (1989); M. C. Marchetti and D. R. Nelson, *Physica (Amsterdam)* **174C**, 40 (1991).  
 [11] R. Busch *et al.*, *Phys. Rev. Lett.* **69**, 522 (1992).  
 [12] I. Giaever, *Phys. Rev. Lett.* **15**, 825 (1965); J. W. Ekin *et al.*, *Phys. Rev. B* **9**, 912 (1974).  
 [13] H. C. Montgomery, *J. Appl. Phys.* **42**, 2971 (1971).  
 [14] D. A. Huse and S. N. Majumdar, *Phys. Rev. Lett.* **71**, 2473 (1993).  
 [15] We have used a two-dimensional infinite slab approximation to obtain by an image method the potential distribution inside the sample. The validity of such an approximation is justified since the contact covers almost the whole sample width and are far away ( $\sim 300 \mu\text{m}$ ) from the edge in the other direction. This approximation yields

$$V_{23}(I_{14})/V_{67}(I_{14})$$

$$= \frac{\ln\{\cosh(D_{12}/x_{\text{eff}}) - 1\}/\{\cosh(D_{13}/x_{\text{eff}}) - 1\}}{\ln\{\cosh(D_{12}/x_{\text{eff}}) + 1\}/\{\cosh(D_{13}/x_{\text{eff}}) + 1\}},$$

and

$$V_{48}(I_{15})/V_{26}(I_{15})$$

$$= \frac{\ln\{\cosh(D_{14}/x_{\text{eff}}) + 1\}/\{\cosh(D_{14}/x_{\text{eff}}) - 1\}}{\ln\{\cosh(D_{12}/x_{\text{eff}}) + 1\}/\{\cosh(D_{12}/x_{\text{eff}}) - 1\}},$$

where  $D_{ab}$  is the distance between contacts  $a$  and  $b$ , and  $x_{\text{eff}} = (D_{15}/\pi)(\rho_c/\rho_{ab})^{1/2}$ .

- [16] In particular, a nonlinearity in the  $c$  axis resistivity could mimic the above behavior. This has been explicitly checked for experimentally and all of the data shown in Fig. 4 are well within the linear response regime. Typical current densities used for that data were  $0.02 \text{ A/cm}^2$ . Nonlinearities were directly measured to set in at current densities of  $\sim 2 \text{ A/cm}^2$  or roughly 2 orders of magnitude higher currents.  
 [17] W. R. White, A. Kapitulnik, and M. R. Beasley, *Phys. Rev. Lett.* **66**, 2826 (1991).  
 [18] W. K. Kwok *et al.*, *Phys. Rev. Lett.* **64**, 966 (1990).  
 [19] L. Civale *et al.*, *Phys. Rev. Lett.* **67**, 648 (1991).